Electrostatic and Hydrophobic Forces Tether the Proximal Region of the Angiotensin II Receptor (AT_{1A}) Carboxyl Terminus to Anionic Lipids†

Henriette Mozsolits,‡ Sharon Unabia,‡ Ariani Ahmad,‡ Craig J. Morton,‡ Walter G. Thomas,§ and Marie-Isabel Aguilar*,‡

Department of Biochemistry and Molecular Biology, P.O. Box 13D, Monash University, Clayton 3800, Victoria, Australia, and The Baker Medical Research Institute, P.O. Box 6492, Saint Kilda Road Central, Melbourne 8008, Australia

Received December 20, 2001; Revised Manuscript Received April 24, 2002

ABSTRACT: The carboxyl terminus of the type-1 angiotensin II receptor (AT_{1A}) is a focal point for receptor activation and deactivation. Synthetic peptides corresponding to the membrane-proximal, first 20 amino acids of the carboxyl terminus adopt an α-helical conformation in organic solvents, suggesting that the secondary structure of this region may be sensitive to hydrophobic environments. Using surface plasmon resonance, immobilized lipid chromatography, and circular dichroism, we examined whether this positively charged, amphipathic α-helical region of the AT_{1A} receptor can interact with lipid components in the cell membrane and thereby modulate local receptor attachment and structure. A synthetic peptide corresponding to the proximal region of the AT_{1A} receptor carboxyl terminus (Leu^{305} to Lys^{325}) was shown by surface plasmon resonance to bind with high affinity to the negatively charged lipid, dimyristoyl L-α-phosphatidyl-DL-glycerol (DMPG), but poorly to the zwitterionic lipid, dimyristoyl L-α-phosphatidylcholine (DMPC). In contrast, a peptide analogue possessing substitutions at four lysine residues (corresponding to $Lys^{307,308,310,311}$) displayed poor association with either lipid, indicating a crucial anionic component to the interaction. Circular dichroism analysis revealed that both the wild-type and substituted peptides possessed α-helical propensity in methanol and trifluoroethanol, while the wild-type peptide also adopted partially inserted helical structure in DMPG and DMPC liposomes. In contrast, the substituted peptide exhibited spectra that suggested the presence of *β*-sheet and α-helical structure in both liposomes. Immobilized lipid chromatography was used to characterize the hydrophobic component of the membrane interaction, and the results demonstrated that hydrophobic and electrostatic interactions mediated the binding of the wild-type peptide but that the substituted peptide bound to the model membranes mainly via hydrophobic forces. We propose that, in intact AT_{1A} receptors, the proximal carboxyl terminus associates with the cytoplasmic face of the cell membrane via a high-affinity, anionic phospholipid-specific tethering that serves to increase the amphipathic helicity of this region. Such associations may be important for receptor function and common for G protein-coupled receptors.

Receptors that activate heterotrimeric guanyl nucleotide binding proteins (G proteins[1]) are a large superfamily with a structure comprising an extracellular amino terminus, seven transmembrane-spanning α-helices (TM1-TM7) connected by alternating extracellular and intracellular loops, and a cytoplasmic carboxyl terminal region (*1*). The arrangement of the seven transmembrane-spanning helices and the extracellular domains provides a specific binding site for ligands, which induces a conformational change in the receptor that exposes intracellular regions, which recruit and activate G proteins. The activated receptor is then phosphorylated and internalized to terminate signaling.

The type-1 angiotensin receptor (AT_{1A}) is a 359 amino acid G protein-coupled receptor (GPCR) that mediates the important cardiovascular and homeostatic actions of the peptide hormone, angiotensin II (AngII) (*2*). The 54 amino acid intracellular carboxyl terminus (Leu^{305} to Glu^{359}) of the AT_{1A} receptor interacts with and activates G proteins (*3*, *4*) and other signaling molecules (*5*−*9*), indicating a contribution to receptor activation, while the discovery of phosphorylation sites (*10*, *11*) and internalization motifs (*12*−*15*) suggest an involvement in receptor regulation. In particular, the proximal region (Leu^{305} to Pro^{321}), comprising the first third of the AT_{1A} carboxyl-terminus, is a site of complex interactions important for receptor function. For example, synthetic peptides corresponding to this region are able to bind and activate purified G proteins (*4*, *16*) and to bind with high affinity to the calcium-regulated effector protein,

† The financial support of Monash University, The National Heart Foundation, and the National Health & Medical Research Council of Australia is gratefully acknowledged.

* Corresponding author. Telephone: 61-3-9905-3723. Facsimile: 61-3-9905-5882. E-mail: mibel.aguilar@med.monash.edu.au.

‡ Monash University.

§ The Baker Medical Research Institute.

[1] Abbreviations: AngII, angiotensin II; AT_{1A}, type-1A AngII receptor; DMPG, dimyristoyl L-α-phosphatidyl-DL-glycerol; DMPC; dimyristoyl L-α-phosphatidylcholine; G proteins, heterotrimeric guanyl nucleotide-binding protein; GPCR, G protein-coupled receptor; NMR, nuclear magnetic resonance; SUV, small unilamellar vesicles; TM1−7, transmembrane-spanning α-helices 1−7; AT, peptide corresponding to residues 305−325 of the AT_{1A} receptor; LGJ, AT peptide containing norleucine substitutions for lysine; CD, circular dichroism.

10.1021/bi0121813 CCC: $22.00
Published on Web 05/22/2002

Table 1: Amino Acid Sequence and Physical Properties of Synthetic Peptides Used in This Study[a]

peptide	sequence	molecular mass	average hydrophobicity	hydrophobic moment
KWL	KWL	445.6	1.39	−
AT	LGKKFKKYFLQLLKYIPPKAK	2551.5	0.93	1.04
LGJ	LGJJFJJYFLQLLKYIPPKAK	2491.1	1.95	0.51

[a] Norleucine (J) substitutions to $Lys^{307,308,310,311}$ (positions 3, 4, 6, and 7 of the AT peptide) are underlined.

calmodulin (*9*). Integrity of this region is also important for receptor internalization (*14*) and coupling to G protein activation and signaling (*4*, *17*). Moreover, fusion proteins of the AT_{1A} carboxyl-terminus and immunoprecipitated AT_{1A} receptors interact with Jak2, STAT proteins, the tyrosine phosphatase SHP-2, and phospholipase Cγ via a $Tyr^{319}Ile^{320}$-$Pro^{321}Pro^{321}$ motif located within the proximal carboxyl terminus (*6*, *7*). What remains poorly defined are the dynamics, hierarchy, and structural requirements for these interactions and activities at the proximal carboxyl terminus.

For some GPCRs, acylation (e.g., palmitoylation) of cysteine residues within the carboxyl terminus, and the subsequent insertion of the acyl group into the lipid bilayer, is a dynamic, agonist-regulated process that serves to tether the cytoplasmic tail to the inner face of the cell membrane (*18*, *19*). Often such acylated cysteines are located 15−20 amino acids from the end of TM7, yielding a short fourth cytoplasmic loop, shown recently in the crystal structure of rhodopsin to be an α-helix (helix VIII) that lies parallel to the membrane face (*20*, *21*). Mutation of such cysteines prevents acylation and can disrupt receptor signaling, internalization, and desensitization (*18*, *19*). In contrast, many GPCRs, including the AT_{1A} receptor, do not contain appropriately placed cysteines and/or are not acylated, either basally or following stimulation. Interestingly, computer-based structural predictions (*14*) and nuclear magnetic resonance (NMR) of synthetic peptides in the organic solvent, trifluoroethanol (TFE) (*22*), suggest that the membrane-proximal region of the AT_{1A} receptor can adopt an amphipathic α-helical conformation, consistent with the rhodopsin structure. Moreover, the corresponding region from the turkey β_1-adrenergic receptor is α-helical in TFE and phospholipid micelles and liposomes (*23*). It is well established that some peripheral membrane proteins (e.g., myristoylated alanine-rich C-kinase substrate (MARCKS) protein; *24*, *25*) can reversibly associate with the cell membrane via so-called amphitropic interactions between charged patches on the protein and the membrane lipids (*26*). Hence, we hypothesized that the carboxyl termini of some GPCRs may be tethered, in the absence of acylation, through interactions between amino acid side chains in this α-helical sequence of the receptor and charged and hydrophobic groups on the membrane lipids.

We have used synthetic peptides and model membranes to show that the proximal amphipathic α-helical region of the AT_{1A} receptor carboxyl terminus binds with high affinity to phospholipid bilayers via both electrostatic and hydrophobic interactions. Thus, this α-helical region is more likely tethered to the plasma membrane rather than extending into the cytoplasm. Many GPCRs possess similar, putative helical extensions from TM7, indicating that, in the absence of acylation on cysteine residues, some receptor tails may dynamically attach to the membrane through side-chain−lipid interactions to regulate local receptor structure and function.

EXPERIMENTAL PROCEDURES

Chemicals and Reagents. HPLC-grade methanol was obtained from Mallinckrodt Baker Inc. (Paris, KY), and water was quartz-distilled and deionized in a Milli-Q system (Millipore, Bedford, MA). 3-[(3-Cholamidopropyl)-dimethylammonio]-1-propanesulfonate (CHAPS), dimyristoyl L-α-phosphatidylcholine (DMPC), and dimyristoyl L-α-phosphatidyl-DL-glycerol (DMPG) were purchased from Sigma (St Louis, MO). A peptide corresponding to amino acids 305−325 of the AT_{1A} receptor (referred to as AT) and an analogue where lysine residues at 307, 308, 310, and 311 were substituted with norleucine (referred to as LGJ) were purchased from Chiron (Clayton, Australia). The control tripeptide (KWL), was synthesized by solid-phase peptide synthesis, purified by reversed-phase high-performance liquid chromatography (RP-HPLC) and characterized by electrospray mass spectrometry. The sequence and molecular mass of AT_{1A} receptor carboxyl-terminal peptides, analogues, and control peptides are listed in Table 1. Also listed in Table 1 are the helical hydrophobic moments for each peptide, calculated according to Eisenberg et al. (*27*) as described previously using amino acid hydrophobicity coefficients derived with C18 RP-HPLC sorbents (*28*). The hydrophobicity value of norleucine was assumed to be equivalent to that of isoleucine.

Liposome Preparation. Small (50 nm) unilamellar vesicles (SUV) of DMPC or DMPG were prepared in 0.02 M phosphate buffer by sonication and extrusion. Dry DMPC was dissolved in ethanol-free chloroform, or, in the case of DMPG, the dry lipid was dissolved in $CHCl_3$/MeOH mixture (2:1, v/v). In both cases, the solvents were evaporated under a stream of nitrogen, and the lipids were held under vacuum overnight. The lipids were resuspended in 0.02 M phosphate buffer, via vortex mixing. The resultant lipid dispersion (a concentration of 0.5 mM with respect to phospholipid) was sonicated and extruded 17 times through polycarbonate filters to obtain SUV at 50 nm size (LiposoFast, pore diameter 50 nm) and used to prepare the lipid bilayer system.

Biosensor Analysis. Biosensor experiments were carried out with a BIACORE X analytical system using the Pioneer L1 sensor chip (Biacore AB, Uppsala, Sweden) at an operating temperature of 25 °C. The Pioneer L1 sensor chip is composed of alkyl chains covalently linked to a dextran-coated gold surface. The running buffer was phosphate buffer (0.02 M NaH_2PO_4/Na_2HPO_4, pH 6.8), the washing solution was 40 mM CHAPS, and the regeneration solution was 10 mM sodium hydroxide. All solutions were freshly prepared, degassed, and filtered through a 0.22 μm filter.

The BIACORE X instrument was cleaned extensively and left running overnight using Milli-Q water to remove trace

amounts of detergent. The surface of the L1 Sensor Chip was cleaned by an injection of the nonionic detergent 40 mM CHAPS (25μL) at a flow rate of 5 μL/min. SUV (80 μL, 0.5 mM) was applied to the sensor chip surface at a flow rate of 2μL/min, and the liposomes were captured on the surface of the sensor chip by the lipophilic compounds and provided a supported lipid bilayer. To remove any multilamellar structures from the lipid surface, we injected sodium hydroxide (30 μL, 10mM) at flow rate of 50 μL/min, which resulted in a stable baseline corresponding to the immobilized liposome bilayer membrane.

Peptide solutions were prepared by dissolving each peptide in 0.02 M phosphate buffer (pH 6.8) from 5 to 40 μM. The solutions (80 μL, 980 s) were injected over the lipid surface at a flow rate of 5 μL/min. The peptide solution was replaced by 0.02 M phosphate buffer (pH 6.8) and the peptide−liposome complex allowed to dissociate for 1200 s. The immobilized liposomes were then removed with an injection of 40 mM CHAPS, and each peptide-membrane association was performed on a freshly prepared liposome surface. All binding experiments were carried out at 25 °C. The affinity of the peptide−lipid binding event was estimated from analysis of a series of response curves. In each case, the resultant sensorgrams were collected at eight different peptide concentrations injected over each lipid surface for each peptide. The peptide concentrations ranged from 5 to 40 μM for binding experiments on DMPC- and DMPG-immobilized liposome surfaces.

The sensorgrams for each peptide−lipid interaction were analyzed by curve fitting using numerical integration analysis. The data were fitted globally by simultaneously fitting the peptide sensorgrams obtained in duplicate at eight different concentrations ranging from 5 to 40 μM. The two-state reaction model was applied to the resultant peptide binding curves to estimate the association and dissociation rate constants. This model was chosen on the basis of previous studies of peptide−membrane interactions (*29*, *30*) and describes two reaction steps, which in terms of peptide−lipid interaction may correspond to

$$P + L \Leftrightarrow PL \Leftrightarrow PL^* \quad (1)$$

where

(1) the peptide (P) binds to lipids (L) to give PL, and

(2) the complex PL changes to PL*, which cannot dissociate directly to P + L and which may correspond to the insertion of the peptide into the lipid bilayer.

The corresponding differential rate equations for this reaction model are represented by

$$dR_1/dt = k_{a1}\cdot C_A\cdot(R_{max} - R_1 - R_2) - k_{d1}\cdot R_1 - k_{a2}\cdot R_1 + k_{d2}\cdot R_2 \quad (2)$$

$$dR_2/dt = k_{a2}\cdot R_1 - k_{d2}\cdot R_2 \quad (3)$$

Circular Dichroism Measurements. CD measurements were carried out on a Jasco J-810 Circular Dichroism Spectropolarimeter (Jasco Corp., Tokyo, Japan) between 190 and 250 nm using quartz cells of 0.1 cm path length at 25 °C. The cell temperature was stabilized using a thermostatic water bath. The scan speed was 20 nm/min, the bandwidth was 1.0 nm, and the resolution was 0.1 nm, with 1 s response. The CD instrument was calibrated with D-10-camphorsulfonic acid. The DMPC and DMPG liposomes were prepared, and the concentration of the lipid solutions was 2 mM. The CD spectra of each peptide were measured in 0.02 M phosphate buffer (pH 6.8) and, in the presence of DMPC or DMPG vesicles, at a peptide concentration of 20 μM. Peptide concentrations were determined using a Hewlett-Packard 845x UV−visible ChemStations spectrophotometer at 280 nm in phosphate buffer. The peptide concentration was determined spectrophotometrically from the tyrosine absorbance using $\epsilon_{280} = 2920\ M^{-1}cm^{-1}$ (based on two tyrosines in each peptide). The peptide-to-lipid ratio was 1:100. In all measurements, CD spectra of the same buffer and/or liposome solutions without peptides were applied as baseline. To obtain final CD spectra, we accumulated the average of five CD scans for each sample and evaluated the results using Jasco Spectra Manager. The helicity of the peptides was determined from the mean residues ellipticity at 222 nm ($[\theta]_{222}$ deg cm^2 dmol^{-1}) according to the relation $[\alpha] = 100^*-[\theta]_{222}/\theta_f$ and $\theta_f = -39500^*(1 - 2.57/n)$, where $[\alpha]$ is the amount of helix, n is the number of residues in the peptides, and θ_f is the mean residues ellipticity of a helix of infinite residues (*31*).

For oriented CD spectra, 0.3 mg of lipid and an amount of peptide (~0.01 mg) to give the desired peptide-to-lipid molar ratio (P/L) of 1:100 were hydrated in 200 μL of milli-Q water, vortexed, and sonicated until visibly clear. The peptide−lipid solution was then deposited onto the inner face of a clean, dry quartz cuvette and kept undisturbed during evaporation of excess water under a nitrogen flow. Measurements were carried out at 25 °C on the Jasco J-810 Circular Dichroism Spectropolarimeter (Jasco Corp., Tokyo, Japan).

HPLC Apparatus. All chromatographic measurements were performed on a Hewlett-Packard 1100 chromatographic system (Agilent Technologies, CA) equipped with a column compartment allowing temperature control. All chromatographic profiles were monitored at 214 nm. Bulk solvents and mobile phases were filtered through a 0.22 μm nylon membrane filter (Alltech Associates, Pty. Ltd. Australia) using a Millipore solvent filtration apparatus (Millipore, Bedford, MA).

Chromatographic Binding Studies. Immobilized phosphatidylglycerol and phosphatidylcholine model membrane surfaces were prepared as previously reported (*32*, *33*). The lipid density was determined from elemental analysis to be 1.08 μmol/m^2, which is similar to the estimated lipid density in biological membranes (*32*). The modified silica was packed into a stainless steel cartridge with dimensions of 4 cm × 4.6 mm ID. The interaction of peptides with the immobilized model membrane was monitored using isocratic elution conditions from 0% to 50% (v/v) methanol in milli-Q water as the mobile phase. A flow rate of 1 mL/min was used throughout, and experiments were carried out at column temperatures of 5, 15, 25, 35, 45, and 55 °C. Peptide solutions were prepared by dissolving the solute at concentrations of 0.1 mg/mL in milli-Q. A 50 μL injection volume was used for all measurements.

The binding of solutes to the immobilized phosphatidylcholine or phosphatidylglycerol monolayers under isocratic elution conditions can be evaluated by the capacity factor, k', according to the following expression:

$$k' = (t_r - t_0)/t_0 \quad (4)$$

where t_r is the retention time of the test compound and t_0 corresponds to the column dead time or void volume. Under conditions where hydrophobic interactions are the dominant interactive force, a linear relationship is generally observed between log k' and φ, the mole fraction of organic solvent required to elute the solute from the hydrophobic surface according to

$$\log k' = \log k_o - S\varphi \quad (5)$$

where log k_o is the capacity factor in the absence of organic solvent and S is the slope of plots of log k' versus φ. The capacity factor, k', can then be related to the equilibrium coefficient, K, of a solute that distributes between the immobilized lipid monolayer and the solvent by the following:

$$k' = \Phi K \quad (6)$$

where the phase ratio, Φ, is the ratio of the volume of the immobilized phospholipids on the silica surface to the total volume of the solvent within the chromatographic column (*32*, *34*).

Peptides and proteins interact with phospholipid surfaces in an orientation-specific manner via a specific contact area. However, when changes in this hydrophobic contact area occur as a result of conformational or orientational effects, changes in the binding affinity, and hence log k', of the peptide are observed. As a consequence, the log k' value is a physical parameter that is highly sensitive to the conformational status of the peptide or protein upon interaction with hydrophobic surfaces (*35*−*40*). In addition, variation of the temperature allows further information to be gained on the effect of peptide conformation and lipid mobility on membrane interactions. The log k' value therefore represents an important probe of changes in peptide orientation during their interaction with the immobilized lipid monolayer as a function of peptide or lipid conformation (*32*, *34*).

All data points were derived from duplicate measurements with retention times between replicates varying by less than 5%. The column dead volume (t_o) was taken as the retention volume of the initial breakthrough peak and was found to be 0.46 min. The phase ratio for the phosphatidylcholine and phosphatidylglycerol monolayers were determined, as previously described (*32*, *33*), to be 0.036 and 0.037, respectively. All interactive parameters were calculated using Excel version 7.0.

Sequence Alignment and Molecular Modeling. Sequences corresponding to the proximal carboxyl termini of a number of GPCRs were aligned using the tinyGRAP database (*41*, *42*). Secondary structure predictions were determined using the automated server PHDsec (www.embl-heidelberg.de/predictprotein; *43*, *44*).

RESULTS

A helical wheel representation of residues 305−325 of the AT_{1A} receptor reveals a significant helical propensity (hydrophobic moment of 1.04, see Table 1) that segregates into a hydrophobic face and a positively charged face constituting multiple lysine residues (Figure 1B). The recent X-ray crystal structure of rhodopsin revealed that the analogous region in rhodopsin forms an amphipathic helix and is located in a hydrophobic environment (*20*). In the present study, we hypothesized that such an amphipathic α-helical structure in close proximity to the cytoplasmic face of the cell membrane may interact directly with the lipid components of the membrane. To investigate this possibility, we synthesized a peptide corresponding to the proximal region of the AT_{1A} carboxyl terminus (AT, residues 305−325) and investigated whether this peptide would interact with model lipid monolayers and bilayers. The potential role of the cationic face of this amphipathic helix was investigated using a peptide analogue of AT where lysine residues at 307, 308, 310, and 311 were substituted with norleucine (referred to as LGJ). These residues have been previously shown through mutation studies to be important for receptor expression (*45*) and form part of a conserved BBXB motif (where B is a basic amino acid and X is any amino acid), which may be important for G protein binding. Substitution of lysine with norleucine maintains side-chain surface area and hydrophobicity while abrogating the positive charge at these residue positions.

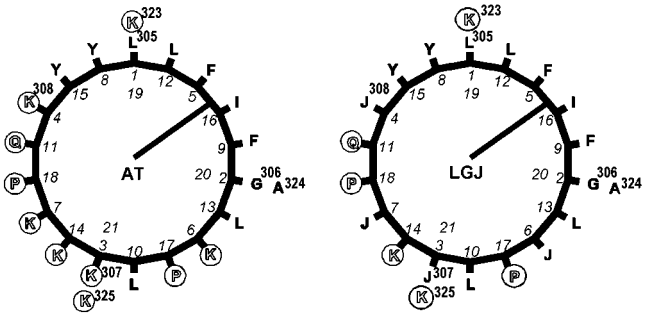

FIGURE 1: Helical wheel representation for the AT and LGJ peptides. Shown are helical wheel plots for the AT and LGJ peptides. Positions 1−21 correspond to residues 305−325 of the AT_{1A} receptor. Hydrophobic residues are represented by the solid letters, while polar residues are indicated by circled letters; J = norleucine. The radial line that points between residues 5 and 16 indicates the direction of the amphipathic moment for both peptides.

Biosensor Studies. Surface plasmon resonance was used to examine the membrane-binding behavior of the AT and LGJ peptides with immobilized liposomes composed of either DMPG or DMPC. Comparative experimental sensorgrams of the binding of each peptide to DMPG and DMPC are shown in Figure 2, together with the sensorgrams obtained at each concentration for both peptides with DMPG and DMPC. There was a proportional increase in the response with increases in peptide concentration, indicating that the system has not reached saturation. Kinetic analysis of the biosensor interactions was subsequently carried out using a two-state model as previously described (*34*, *46*), and the rate constants and association constants are listed in Table 2. This model was selected on the basis of the multistep model of peptide−lipid interactions, which may involve initial electrostatic interaction followed by reorientation and/or insertion of the peptide into the hydrophobic interior. As previously observed for the binding of antimicrobial peptides with DMPC and DMPG, the Langmuir model, which describes a simple one-step 1:1 bimolecular interaction, results in a poor fit for both the association and dissociation phases when used to analyze the binding of peptides to model membranes. In contrast, the two-state model resulted in a significantly improved fit and generated affinity constants that were similar to published data derived using different

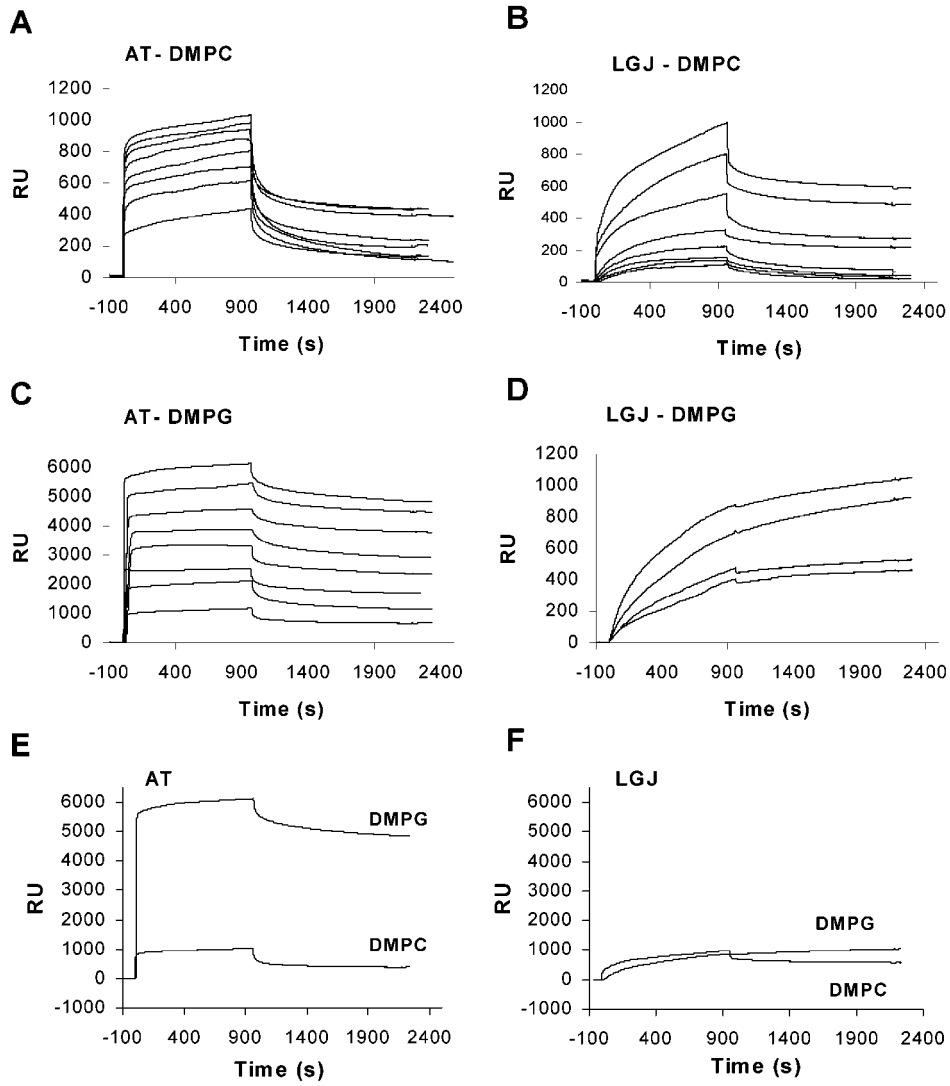

FIGURE 2: Sensorgrams for AT and LGJ peptides binding to DMPG and DMPC liposomes immobilized on the L1 sensor chip surface. Plots of RU (response units) vs time for (A) AT on DMPC, (B) LGJ on DMPC, (C) AT on DMPG, (D) LGJ on DMPG (for panels A−D, peptide concentration = 5−40μM), (E) AT on DMPC and DMPG at 40μM, and (F) LGJ on DMPC and DMPG at 40μM. Injections were made at time = 0 min, and phosphate buffer was added to initiate dissociation at 980 s.

Table 2: Binding Data Determined from Surface Plasmon Resonance (k_{a1}, k_{d1}, k_{a2}, k_{d2}, K_{ass}) and Immobilized Lipid Chromatography t_R)[a]

	rate constants						
lipid/peptide	k_{a1} (1/ms)	k_{d1} (1/s)	k_{a2} (1/ms)	k_{d2} (1/s)	K_{ass} (1/M)	t_R[b] (min)	4σ[b] (min)
			DMPG				
AT	33571.4	0.8×10^{-2}	1.7×10^{-3}	1.9×10^{-4}	403×10^{5}	2.84	1.0
LGJ	–	–	–	–	–	5.60	4.5
			DMPC				
AT	4858.8	4.6×10^{-2}	1.1×10^{-3}	5.6×10^{-4}	2.1×10^{5}	0.71	0.18
LGJ	99.4	0.4×10^{-2}	0.8×10^{-3}	1.3×10^{-4}	1.8×10^{5}	0.67	0.34

[a] Surface plasmon resonance parameters were derived from global fitting of duplicate experimental curves obtained at seven different concentrations. [b] Data obtained at 25 °C and 0% methanol.

techniques (*34*, *46*). Similarly, the 1:1 Langmuir model resulted in a poor fit when used to analyze the binding of AT and LGJ with these lipid surfaces (results not shown), and the two state model was used to analyze the sensorgrams shown in Figure 2A−D.

Analysis of the biosensor curves reveals different binding kinetics with significant disparity in respect to the association and dissociation rates for both peptides (see Table 2). The curves indicate that the AT peptide binds very rapidly to both lipids, but with a 200-fold higher affinity for the anionic DMPG ($K_{ass} = 403 \times 10^5 M^{-1}$) than for the zwitterionic DMPC ($K_{ass} = 2.1 \times 10^5 M^{-1}$). For both lipids, the sensorgrams did not return to the baseline following dissociation (Figure 2), which indicates that a proportion of the peptide remains bound to the lipid membrane, presumably through strong hydrophobic interactions.

The results for LGJ contrasted significantly with the results for the AT peptide. While AT and LGJ had similar K_{ass} values for binding to DMPC, the binding of LJG was associated with a much slower on-rate for the first putative

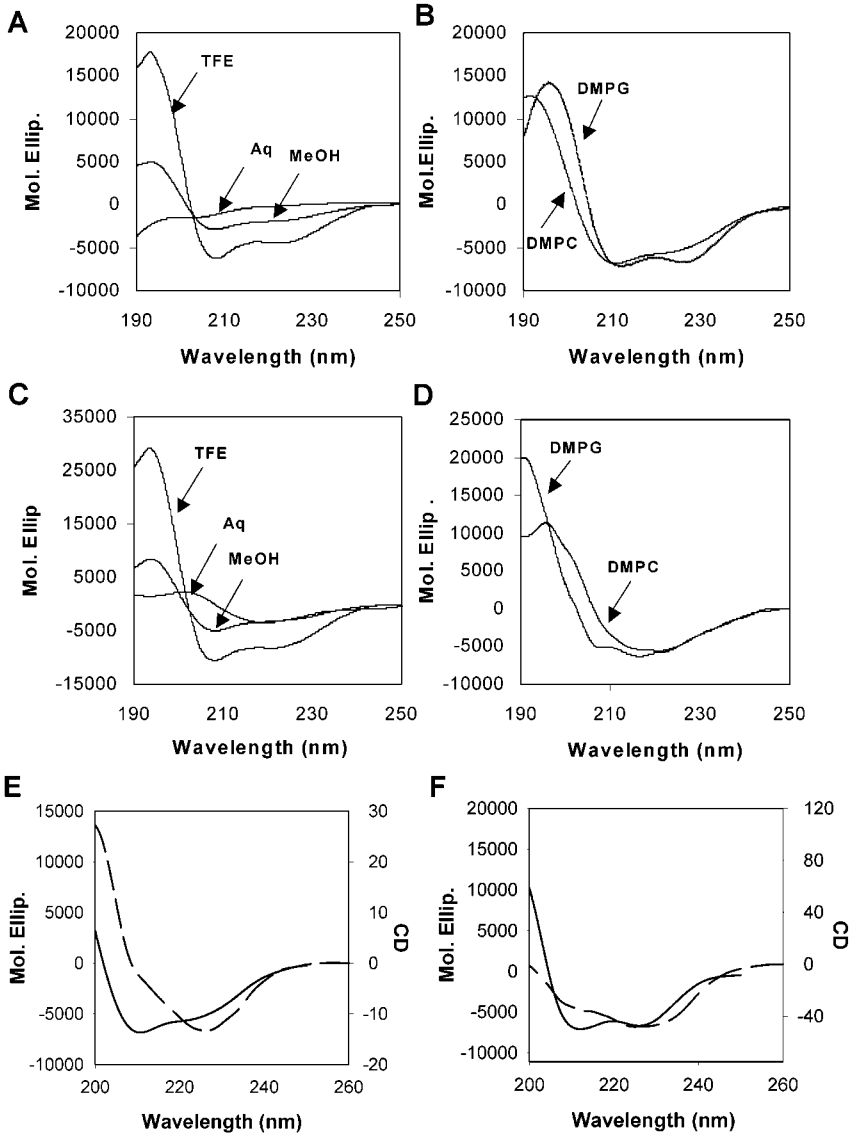

FIGURE 3: CD spectra for AT and LGJ. Panels A and C show spectra for AT and LGJ, respectively, in phosphate buffer, 50% methanol (MeOH), or 50% TFE. Panels B and D, AT and LGJ respectively, were determined in 2mM DMPG or 2mM DMPC liposomes, as indicated. Panels E and F show the oriented spectra obtained for AT (dashed line) superimposed on the conformational spectra (solid line) obtained in DMPC and DMPG, respectively.

binding step (AT, k_{a1}= 4858.8/ms; LGJ, k_{a1}= 99.4/ms). In addition, the sensorgrams for LJG binding to DMPG continued to rise during the dissociation phase, indicating a significant difference in the mode of binding of this peptide with the anionic lipids. This lack of dissociation of LGJ with DMPG is indicative of a very slow irreversible binding—presumably through hydrophobic interactions. As a consequence, kinetic analysis could not be performed to yield association constants. This result also indicates that substitution of the four lysine residues resulted in loss of the specificity of binding to the anionic lipid.

Taken together, these results indicate that the AT peptide initially binds with the anionic phospholipids through a rapid electrostatic interaction via the lysine residues, which is followed by reorientation and/or insertion of the peptide into the hydrophobic interior of the lipid bilayer. The reduced overall binding of LGJ to both phospholipids clearly highlights the prominent role that electrostatic interactions play.

Circular Dichroism & Amphipathicity. To determine if the structure of the AT and LGJ peptides is affected by association with lipid, we next used circular dichroism to determine the conformation of AT and LGJ under various solvent conditions. The CD spectra were obtained in phosphate buffer, 50% methanol, 50% TFE, DMPC liposomes, and DMPG liposomes and are shown in Figure 3A−D. While AT did not adopt any structure in phosphate buffer, there was some evidence of β-sheet structure for LGJ, suggesting some aggregation in phosphate buffer. Both peptides adopted helical structure in 50% methanol (AT, 6%; LGJ, 9%) and 50% TFE (AT, 12%; LGJ, 24%). It has been previously shown (*22*) that a peptide corresponding to residues 300−320 of the AT_{1A} receptor adopted a concentration dependent α-helical structure in water at peptide concentrations of 20−120μM and displayed ~50% helicity at 30% TFE. The lower helical content observed for the AT peptide in the present study most likely reflects the region of receptor sequence chosen (residues 305−325), which

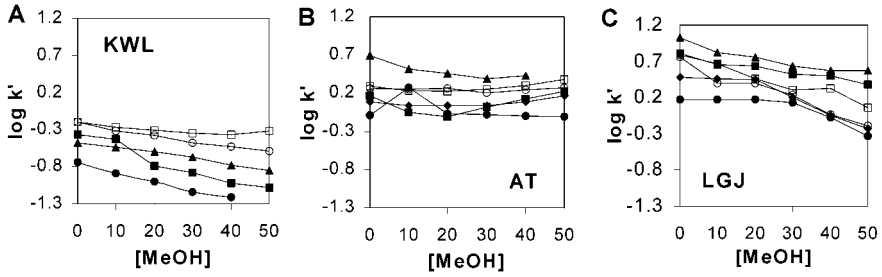

FIGURE 4: Displacement profiles for the peptides KWL, AT, and LGJ using immobilized phosphatidylglycerol chromatography. Plot of log k' vs % methanol (0−50%) at 5 °C (closed circles), 15 °C (closed squares), 25 °C (closed triangles), 35 °C (closed diamonds), 45 °C (open circles), and 55 °C (open squares) for (A) KWL, (B) AT, and (C) LGJ, following elution from the immobilized PG monolayer at 1 mL/min. Log k' was calculated according to eq 4 in Experimental Procedures.

includes two helix-disrupting proline residues (Pro^{321}, Pro^{322}) at the C terminus. The AT peptide also displayed helical structure in DMPG (19%) and DMPC (10%). In contrast, LGJ exhibited spectra which suggested the presence of a mixture of helix and β-sheet in both DMPG and DMPC. These results therefore indicate that the AT peptide binds to lipids in a helical conformation while LGJ adopts a significantly different structure in the presence of lipids. Oriented CD was used to determine the orientation of the AT peptide at the surface of the liposomes, and the oriented spectra are shown together with the unoriented spectra in Figure 3E,F. The results indicate the partial loss of the first minimum at 208 nm in the oriented spectrum for both DMPC and DMPG which, based on previous analyses of oriented CD spectra by others (*47*), corresponds to the partial insertion of the peptide into the phospholipid bilayer. Oriented spectra were not obtained for LGJ due to the complex unoriented spectra observed for this peptide.

Immobilized Lipid Chromatography. Binding Affinity. The binding of the AT and LGJ peptides to lipid was also studied by immobilized lipid chromatography. In this system, modified phosphatidylglycerol (PG) or phosphatidylcholine (PC) was covalently attached to an activated silica (*32*, *33*). Bound peptide is displaced by varying the methanol concentration, which specifically allows the contribution of hydrophobic interactions to the peptide−membrane interaction to be studied. This technique thus complements the surface plasmon resonance experiments by allowing complete dissociation of the bound peptide and quantification of the hydrophobic interactions (*34*).

The binding affinities of each peptide for phospholipid (log k') were derived according to eq 4 (Experimental Procedures) from the isocratic retention times obtained with methanol concentrations between 0% and 50% at a flow rate of 1 mL/min and at temperatures between 5 and 55 °C. The tripeptide KWL was used as a low-molecular-weight control molecule that does not undergo any significant conformational change either in solution or upon adsorption to a hydrophobic surface. Any variation observed in log k' values for this peptide is not related to changes in structure or orientation and location within the lipid monolayer. Figure 4 shows plots of log k' versus methanol percentage ($\varphi \times 100$) for the elution of KWL, AT, and LGJ from the PG monolayer at temperatures ranging from 5 to 55 °C. KWL exhibited a linear decrease in solute retention with increasing methanol concentration (Figure 4A), indicating that hydrophobic interactions were the dominant force in the interaction of this peptide with the PG monolayer. In contrast, the corresponding data for the AT peptide indicated that its retention was largely independent of the methanol percentage and sometimes increased at higher methanol concentrations (Figure 4B). In addition, AT exhibited much higher binding affinities ($-0.11 < \log k' > 0.69$) compared to those of KWL ($-1.21 < \log k' > -0.20$) in all conditions. Since increasing the methanol percentage did not cause a decrease in the retention of AT, the results suggest that dipolar and electrostatic interactions also contribute significantly to the binding of the AT peptide to the immobilized PG monolayer. By comparison, at lower percentages of methanol, the LGJ peptide exhibited a stronger interaction with the immobilized PG ligands, as evident from the higher log k' values (Figure 4C). This reflects the increased hydrophobicity due to the norleucine substitutions. However, the log k' values generally decreased with increasing methanol concentrations, demonstrating that this peptide interacts predominantly through hydrophobic interactions with minimal contributions from electrostatic forces. The absence of the four N-terminal lysine residues in LGJ increases the overall hydrophobicity but decreases the amphipathicity of the peptide (Table 1), which resulted in stronger hydrophobic binding of this analogue to the immobilized lipids. Retention-time data is listed in Table 2 for comparison with the biosensor binding data. For example, at 0% methanol and 25 °C, the retention time for LGJ (5.60 min) was twice that observed for AT (2.84 min). This retention behavior is consistent with the biosensor results, which demonstrated a very slow and irreversible binding of LGJ to the DMPG liposomes.

The binding of KWL, AT, and LGJ to the immobilized PC monolayer was also analyzed and the corresponding plots of log k' versus methanol percentage at 25 and 45 °C are shown in Figure 5. In general, the retention time of KWL was higher on PC than on PG, indicating a stronger hydrophobic interaction of this small peptide with the PC ligands. However, AT and LGJ exhibited lower retention on the PC than on the PG monolayer, confirming that the AT and LJG peptides bind more strongly to the anionic lipids and agreeing with the results obtained using surface plasmon resonance. However, LJG generally exhibited a higher retention than AT, indicating a stronger hydrophobic interaction with the PC monolayer than AT.

The comparative behavior of each peptide on the PG surface was further analyzed through the influence of temperature on the range of retention values as shown in Figure 6. KWL demonstrated a small increase in retention with increasing temperature. While AT also showed a gradual increase in retention with increasing temperature, this peptide

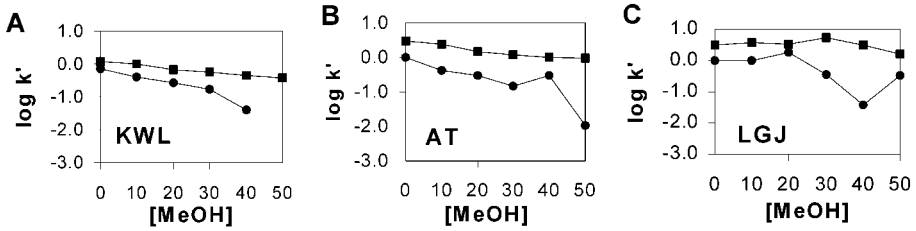

FIGURE 5: Displacement profiles for the peptides KWL, AT, and LGJ using immobilized phosphtidylcholine chromatography. Plot of log k' vs % methanol (0−50%) at 25 °C (closed circles) and 45 °C (closed squares) for (A) KWL, (B) AT, and (C) LGJ following elution from the immobilized PC monolayer at 1 mL/min.

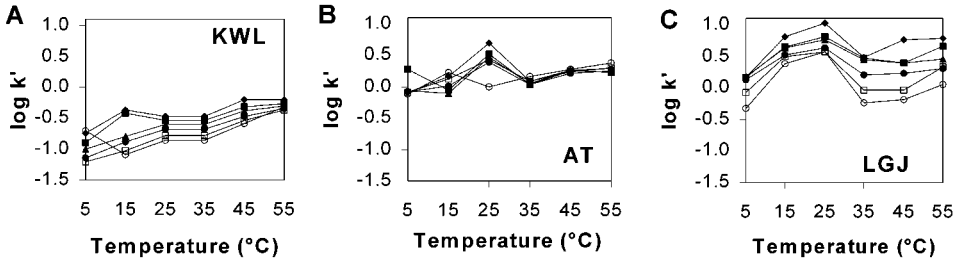

FIGURE 6: Displacement profiles for the peptides KWL, AT, and LGJ using immobilized phosphatidylglycerol chromatography. Plot of log k' vs temperature for (A) KWL, (B) AT, and (C) LGJ following elution from the immobilized PG monolayer at (closed diamonds) 0%, (closed squares) 10%, (closed triangles) 20%, (closed circles) 30%, (open squares) 40%, and (open circles) 50% methanol at 1 mL/min. Log k' was calculated according to eq 4 in Experimental Procedures.

also showed a significant transition in retention at 25 °C, which again corresponds to the monolayer phase transition. Most importantly, further evidence of the difference in binding behavior between AT and LJG is seen by the larger variation in retention over the whole temperature range for LGJ. As the control molecule, KWL, did not exhibit the biphasic retention behavior and CD results indicated that both peptides adopted some helical structure in 50% methanol and in DMPG liposomes, the results suggest that AT and LGJ undergo conformational changes during the interaction with the PG monolayer, which is reflected in changes in lipid affinity and/or insertion into the lipid monolayer. The larger variation in retention values for LGJ demonstrates that the degree of reorientation and insertion is significantly different between these peptides. The corresponding data for the binding of the peptides to the PC monolayer showed very little difference in the behavior of each peptide (data not shown). These results further demonstrate the loss of selectivity of binding of the control and the test peptides to the PC surface.

Bandwidth Changes. The interactive behavior of solutes with the immobilized lipid monolayer was also assessed through analysis of elution peak widths. The experimentally observed bandwidth for small, rigid organic molecules that interact through a single binding site and a unique orientation in the lipid monolayer appear as a symmetrical peak. In contrast, atypical bandbroadening can be associated with solute conformational interconversions during the interaction with the immobilized phospholipds (*32*, *33*, *40*). The degree of bandbroadening also provides information on the rate of conformational and insertional equilibria upon binding of each peptide to the lipid surface.

The overall dependence of experimental bandwidth (measured at 4σ) on methanol percentage and temperature for KWL, AT, and LGJ was analyzed for both the PG and PC monolayers. Very little variation was observed for KWL for both lipid phases, with 4σ values varying typically between 0.06 and 0.16 min. This result reflects the behavior of the small control molecule that does not undergo changes in secondary structure or the degree of insertion into the lipid monolayer. In contrast, significant variation in 4σ values were obtained for AT and LGJ, with values ranging from 0.2 to 1.8 min and from 0.4 to 4.5 min, respectively. These results indicate that these peptides undergo conformational and orientational changes on a time scale that are comparable to the residence time on the immobilized PG monolayer, i.e., during the course of the experiment (typically < 15 min). In particular, LGJ exhibited a very distinct transition in the bandwidth at 25 °C, which correlated with the temperature at which a change in the log k' plots was observed. Since the 4σ value is dependent on the number of conformational and insertional intermediates present at the lipid surface, these results provide further evidence of the important role of the lysine residues in the binding of the AT peptide with phospholipid surfaces. Specifically, the higher 4σ values observed for LGJ (comparative values are listed in Table 2) indicate that the rate of structure induction and surface reorientation is significantly slower for LGJ than for AT, which is consistent with the slower association and dissociation evident in the biosensor experiments.

Similar bandbroadening results were observed with the PC monolayer, with LGJ exhibiting larger bandbroadening than AT, again reflecting a slower rate of interconversion at the lipid surface. However, the 4σ values for both peptides were much lower on the PC monolayer compared to those on the PG monolayer, reflecting the limited interaction of the peptides with the PC surface.

DISCUSSION

On the basis of computer modeling, we proposed that the proximal carboxyl terminus of the AT_{1A} receptor (residues 305−320) is an amphipathic α-helix and that this structure may be relevant to receptor activation and internalization (*14*). Subsequently, using CD and NMR, Franzoni et al. (*22*) confirmed that peptides derived from this region formed

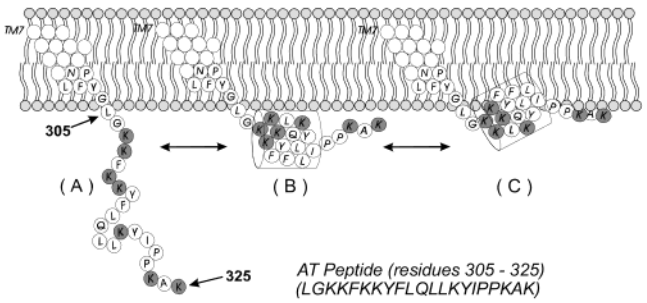

FIGURE 7: Model of the binding of AT peptide to anionic phospholipids in the membrane. The peptide is unstructured in aqueous environments (A) but, upon approach to the membrane, adopts an α-helical conformation, allowing it to bind electrostatically via the lysine residues (B). The peptide then reorientates and partially inserts in the membrane to allow hydrophobic residues to be located in the membrane interior and the lysine residues to reside at the membrane surface (C).

α-helices in the helix-promoting solvent, TFE. The results of the present study using surface plasmon resonance, CD, and immobilized lipid chromatography provide the first evidence that the carboxyl-terminal region of the AT_{1A} receptor binds to anionic phospholipids that are present in the cell membrane and provide some information on the possible mechanism of interaction. We therefore propose a model for the AT_{1A} receptor in which the proximal carboxyl terminus binds to anionic regions of the cell membrane. This occurs first through electrostatic interactions, followed by reorientation and partial insertion of the peptide to allow hydrophobic interactions to anchor the peptide at the interfacial region of the membrane (shown schematically in Figure 7). Removal of four lysine residues ($Lys^{307,308,310,311}$) significantly affected the binding behavior of the AT peptide, resulting in the loss of DMPG-specific binding through elimination of the initial rapid phase of binding associated with electrostatic interactions. Thus, the cytoplasmic region of the AT_{1A} receptor may not extend into the cytoplasm but, rather, is tethered to the cell membrane lipids. This orientation of the helix relative to the membrane is well supported by the recent X-ray structures of bovine and squid rhodopsin (*20*, *21*). At 2.8 Å resolution, the proximal carboxyl terminus (residues 311−321 of bovine rhodopsin), turns sharply, immediately after exiting the membrane after TM7, and forms another helix (helix VIII), which orientates itself parallel to the membrane surface. Sequence alignment reveals that residues 307−317 in the AT_{1A} receptor correspond to the C-terminal helix VIII in rhodopsin. It is not clear from the bovine rhodopsin structure whether the side chains on helix VIII contact or engage the membrane lipids, although it was suggested by the authors that they are located in a hydrophobic environment, presumably involving peptide−peptide as well as peptide−lipid interactions. The position of the acylated cysteines in rhodopsin (residues 322 and 323) may be tethering helix VIII to the membrane. In contrast, we predict that for nonacylated receptors, amphitropic interactions may provide an important alternative mechanism for dynamic tethering.

One of our major findings is that the proximal AT_{1A} carboxyl terminus binds with high selectivity to anionic membrane lipids. A range of techniques has demonstrated that there is an asymmetric distribution of anionic phospholipids in mammalian and viral membranes (*48*). For example, it has been shown (*49*) that approximately 85% of the anionic phosphatidylserine is located on the cytosolic side of the human plasma membrane. Indeed, the cytoplasmic face of the plasma membrane is rich in acidic lipids (~30%) (*26*), and this transverse membrane asymmetry results in a net negative charge at the cytosolic face at physiological pH. This charged surface provides a binding site for cationic regions of amphitropic proteins and possibly the carboxyl-terminal regions of receptors such as AT_{1A} and rhodopsin. While we have identified a strong association of the proximal carboxyl terminus with phosphatidylglycerol, further studies with mixtures of anionic and zwitterionic lipids are required to determine the capacity of this region to associate with other acidic lipids, including those generated (e.g., polyphosphoinositides and phosphatidic acid) during signal generation.

Our data can be most directly compared to the study of Jung et al. (*23*). This group used CD and NMR-based approaches to show that a peptide (T345−359), derived from the avian β-adrenergic receptor and capable of inhibiting adenylate cyclase activity, can adopt a strongly α-helical conformation in TFE as well as in phospholipid micelles and vesicles. This region of the β-adrenergic receptor was predicted to orientate itself parallel to the membrane in a manner analogous to that of mastoparan, a peptide derived from wasp venom that also inhibits receptor-G protein coupling. Like rhodopsin, the β-adrenergic receptor is reversibly palmitoylated, and this may strengthen and/or modify membrane attachment. Taken together with the present study, these data suggest that the tethering and structure of helix VIII may be common for GPCRs. In Table 3, a comparison of sequences corresponding to the proximal carboxyl terminus for a selection of GPCRs is shown. With reference to the highly conserved NPXXY motif at the end of transmembrane helix 7, there are often basic or charged residues surrounding a highly conserved phenylalanine (Phe^{309} in AT_{1A}) as well as other conserved hydrophobic residues in sequences that clearly display helical propensity. The identification of phenylalanine as a preferred interfacial anchoring amino acid (*50*) may explain its conservation within the proximal carboxyl termini of GPCRs.

Amphitropism by the proximal carboxyl terminus of the AT_{1A} receptor and other GPCRs may contribute to receptor function in a number of ways. Our CD data indicate an increased helical content of the AT peptide in the presence of DMPG, which suggests that lipid binding by the proximal carboxyl terminus may promote local structures necessary for interaction with disparate signaling and regulatory molecules. This may involve correct positioning of the proximal carboxyl terminus relative to other cytoplasmic loops of the receptor or by orientation of the carboxyl-terminus helix within the membrane that exposes key charged residues to the cytoplasm and interacting molecules. Alternatively, helix VIII of GPCRs may be acting as sensors or modifiers of local lipid composition. Indeed, a recent study has shown that membrane composition influences the kinetics of the binding of transducin to rhodopsin and is thus a critical factor in determining the temporal response of G-protein-coupled signaling systems (*51*). Given that different membrane lipids are concentrated in discrete compartments of the plasma membrane, specific lipid binding domains in GPCR carboxyl termini may localize receptors to particular

Table 3: Alignment of Amino Acid Sequences Corresponding to the Proximal C-Terminal Regions of Selected Family A GPCRs[a]

GPCR	Swiss Prot. No.	Sequence	Hydrophobic Moment
Consensus Sequence		NPϕϕY_Fϕ_+_F++__ϕ_ϕϕ I	
AT_{1A}	P25095	NPLFYGFLGKKFKKYFLQLLKYIPPKAK hhhhhhhhhhhhh	0.76
LHCG	P22888	NPFLYAIFTKTFQRDFFLLLSKFG hhhhhhhhhhhhh	0.57
TSH	P16473	NPFLYAIFTKAFQRDVFILLSKFGI hhhhhhhhhhhhh	0.35
FSH	P23945	NPFLYAIFTKNFRRDFFILLSK hhhhhhhhhh	0.41
IL8a	P25024	NPIIYAFIGQNFRHGFLKILAMHG hhhhhhhhhhhh	0.26
SRIF2A	P30872	NPILYGFLSDNFKRSFQRILCLSWM hhhhhhhhhhhh	0.46
Y1NPY	P25929	NPIFYGFLNKNFQRDLQFFFNFCD hhhhhhhhhhhhh	0.68
A1AA	P35348	NPIIYPCSSQEFKKAFQNVLRIQ hhhhhhhhhhh	0.52
A1AB	P35368	NPIIYPCSSKEFKRAFVILGC hhhhhhhhhh	0.45

[a] Alignments begin with the highly conserved NPXXY motif at the end of transmembrane 7 [ϕ = hydrophobic, + = basic]. Also listed are the consensus sequence, hydrophobic moments and regions of helical propensity (h).

regions, allowing interaction with similarly located signaling/regulatory molecules. Finally, given that amphitropism is known to be regulated by protein modification such as phosphorylation and by protein−protein interactions, the interaction between the AT_{1A} receptor carboxyl terminus and membrane lipids may be similarly regulated. For example, MARCKS and the signaling kinase Src are amphitropic proteins that use both myristoylation and polybasic motifs to reversibly associate with the plasma membrane (*26*). The electrostatic association afforded by the polybasic motif can be disrupted by competitors, such as calmodulin, which bind and mask the polybasic membrane-binding site or by phosphorylation, both within and adjacent to this motif. Phosphorylation presumably competes with the acidic lipids for binding to the positively charged amphipathic helix and dramatically lowers the affinity of Src for lipid vesicles and increases its cytoplasmic distribution (*52*). Recently, we reported the high-affinity interaction of calmodulin with the proximal carboxyl terminus of the AT_{1A} receptor (*9*), highlighting the possibility of an analogous mechanism of regulation. Moreover, it is well established for the AT_{1A} receptor (and many other GPCRs) that the carboxyl terminus adjacent to the proximal helical region is robustly phosphorylated following receptor activation (*10, 11*). Hence, competition may well exist between acidic lipids in the membrane and phosphorylated residues in the distal carboxyl terminus for binding to the proximal carboxyl terminus. Such possibilities merit further investigation.

In summary, we report the selective binding of a peptide derived from the proximal region of the AT_{1A} receptor carboxyl terminus to anionic lipids, which promotes the amphipathic α-helical structure of this peptide. Our data are consistent with a two-step process: an initial electrostatic interaction, followed by reorientation and intercalation of the hydrophobic groups into the phospholipid interior. In this regard, the binding process is reminiscent of the reversible association of amphipathic helices from other amphitropic proteins with membranes (*26*). Given that many GCPRs possess analogous putative amphipathic helical sequences within the carboxyl-terminus region, this structure and its modulation by lipid binding may represent a common mechanism for modifying GPCR signaling and regulation.

ACKNOWLEDGMENT

We thank Dr Maurits dePlanque for helpful discussions with the oriented CD data.

REFERENCES

1. Vaughan, M. (1998) *J. Biol. Chem. 273*, 17297.
2. de Gasparo, M., Catt, K. J., Inagami, T., Wright, J. W., and Unger, T. (2000) *Pharmacol. Rev. 52*, 415−72.
3. Ohyama, K., Yamano, Y., Chaki, S., Kondo, T., and Inagami, T. (1992) *Biochem. Biophys. Res. Commun. 189*, 677−83.
4. Sano, T., Ohyama, K., Yamano, Y., Nakagomi, Y., Nakazawa, S., Kikyo, M., Shirai, H., Blank, J. S., Exton, J. H., and Inagami, T. (1997) *J. Biol. Chem. 272*, 23631−6.
5. Marrero, M. B., Schieffer, B., Paxton, W. G., Heerdt, L., Berk, B. C., Delafontaine, P., and Bernstein, K. E. (1995) *Nature 375*, 247−50.
6. Ali, M. S., Sayeski, P. P., Dirksen, L. B., Hayzer, D. J., Marrero, M. B., and Bernstein, K. E. (1997) *J. Biol. Chem. 272*, 23382−8.
7. Marrero, M. B., Venema, V. J., Ju, H., Eaton, D. C., and Venema, R. C. (1998) *Am. J. Physiol. 275*, C1216−23.

8. Daviet, L., Lehtonen, J. Y., Tamura, K., Griese, D. P., Horiuchi, M., and Dzau, V. J. (1999) *J. Biol. Chem. 274*, 17058−62.
9. Thomas, W. G., Pipolo, L., and Qian, H. (1999) *FEBS Lett. 455*, 367−71.
10. Thomas, W. G., Motel, T. J., Kule, C. E., Karoor, V., and Baker, K. M. (1998) *Mol. Endocrinol. 12*, 1513−24.
11. Smith, R. D., Hunyady, L., Olivares-Reyes, J. A., Mihalik, B., Jayadev, S., and Catt, K. J. (1998) *Mol. Pharmacol. 54*, 935−41.
12. Hunyady, L., Bor, M., Balla, T., and Catt, K. J. (1994) *J. Biol. Chem. 269*, 31378−82.
13. Thomas, W. G., Thekkumkara, T. J., Motel, T. J., and Baker, K. M. (1995) *J. Biol. Chem. 270*, 207−13.
14. Thomas, W. G., Baker, K. M., Motel, T. J., and Thekkumkara, T. J. (1995) *J. Biol. Chem. 270*, 22153−9.
15. Thomas, W. G. (1999) *Regul. Pept. 79*, 9−23.
16. Kai, H., Alexander, R. W., Ushio-Fukai, M., Lyons, P. R., Akers, M., and Griendling, K. K. (1998) *Biochem. J. 332*, 781−7.
17. Parnot, C., Bardin, S., Miserey-Lenkei, S., Guedin, D., Corvol, P., and Clauser, E. (2000) *Proc. Natl. Acad. Sci. U.S.A. 97*, 7615−20.
18. Morello, J. P., and Bouvier, M. (1996) *Biochem. Cell Biol. 74*, 449−57.
19. Milligan, G., Grassie, M. A., Wise, A., MacEwan, D. J., Magee, A. I., and Parenti, M. (1995) *Biochem. Soc. Trans. 23*, 583−7.
20. Palczewski, K., Kumasaka, T., Hori, T., Behnke, C. A., Motoshima, H., Fox, B. A., Le Trong, I., Teller, D. C., Okada, T., Stenkamp, R. E., Yamamoto, M., and Miyano, M. (2000) *Science 289*, 739−45.
21. Davies, A., Gowen, B., Krebs, A. M., Schertler, F. X., and Saibil, H. R. (2001) *J. Mol. Biol. 314*, 455−463.
22. Franzoni, L., Nicastro, G., Pertinhez, T. A., Tato, M., Nakaie, C. R., Paiva, A. C., Schreier, S., and Spisni, A. (1997) *J. Biol. Chem. 272*, 9734−41.
23. Jung, H., Windhaber, R., Palm, D., and Schnackerz, K. D. (1996) *Biochemistry 35*, 6399−405.
24. Kim, J., Shishido, T., Jiang, X., Aderem, A., and McLaughlin, S. (1994) *J. Biol. Chem. 269*, 28214−9.
25. Arbuzova, A., Wang, J., Murray, D., Jacob, J., Cafiso, D. S., and McLaughlin, S. (1997) *J. Biol. Chem. 272*, 27167−77.
26. Johnson, J. E., and Cornell, R. B. (1999) *Mol. Membr. Biol. 16*, 217−35.
27. Eisenberg, D., Weiss, R. M., and Terwilliger, T. C. (1982) *Nature 299*, 371−4.
28. Wilce, M. C. J., Aguilar, M. I., and Hearn, M. T. W. (1995) *Anal. Chem. 67*, 1210−19.
29. Karlsson, R., and Falt, A. (1997) *J. Immunol. Methods 200*, 121−33.
30. Morton, T. A., Myszka, D. G., and Chaiken, I. M. (1995) *Anal. Biochem. 227*, 176−85.
31. Chen, Y. H., Yang, J. T., and Chau, K. H. (1974) *Biochemistry 13*, 3350−9.
32. Mozsolits, H., Lee, T. H., Wirth, H. J., Perlmutter, P., and Aguilar, M. I. (1999) *Biophys. J. 77*, 1428−44.
33. Lee, T.-Z., Rivett, D., Werkmeister, J., Hewish, D., and Aguilar, M. I. (1999) *Lett. Pept. Sci. 6*, 371−80.
34. Lee, T.-Z., Mozsolits, H., and Aguilar, M. I. (2001) *J. Pept. Res.*, 464−476.
35. Zhou, N. E., Mant, C. T., and Hodges, R. S. (1990) *Pept. Res. 3*, 8−20.
36. Blondelle, S. E., Simpkins, L. R., Perez-Paya, E., and Houghten, R. A. (1993) *Biochim. Biophys. Acta 1202*, 331−6.
37. Purcell, A. W., Aguilar, M. I., Wettenhall, R. E., and Hearn, M. T. (1995) *Pept. Res. 8*, 160−70.
38. Krause, E., Beyermann, M., Dathe, M., Rothemund, S., and Bienert, M. (1995) *Anal. Chem. 67*, 252−8.
39. Lazoura, E., Maidonis, I., Bayer, E., Hearn, M. T., and Aguilar, M. I. (1997) *Biophys. J. 72*, 238−46.
40. Steer, D. L., Thompson, P. E., Blondelle, S. E., Houghten, R. A., and Aguilar, M. I. (1998) *J. Pept. Res. 51*, 401−12.
41. Kristiansen, K., Dahl, S. G., and Edvardsen, O. (1996) *Proteins 26*, 81−94.
42. Edvardsen, O., and Kristiansen, K. (1997) *7TM J 6*, 1−6.
43. Rost, B., and Sander, C. (1993) *J. Mol. Biol. 232*, 584−99.
44. Rost, B., and Sander, C. (1994) *Proteins 19*, 55−72.
45. Gaborik, Z., Mihalik, B., Jayadev, S., Jagadeesh, G., Catt, K. J., and Hunyady, L. (1998) *FEBS Lett. 428*, 147−51.
46. Mozsolits, H., Wirth, H. J., Werkmeister, J., and Aguilar, M. I. (2001) *Biochim. Biophys. Acta 1512*, 64−76.
47. de Jongh, H. H., Goormaghtigh, E., and Killian, J. A. (1994) *Biochemistry 33*, 14521−8.
48. Devaux, P. F. (1991) *Biochemistry 30*, 1163−73.
49. Gascard, P., Tran, D., Sauvage, M., Sulpice, J. C., Fukami, K., Takenawa, T., Claret, M., and Giraud, F. (1991) *Biochim. Biophys. Acta 1069*, 27−36.
50. Killian, J. A., and von Heijne, G. (2000) *Trends Biochem. Sci. 25*, 429−34.
51. Mitchell, D. C., Niu, S. L., and Litman, B. J. (2001) *J. Biol. Chem. 276*, 42801−6.
52. Murray, D., Hermida-Matsumoto, L., Buser, C. A., Tsang, J., Sigal, C. T., Ben-Tal, N., Honig, B., Resh, M. D., and McLaughlin, S. (1998) *Biochemistry 37*, 2145−59.

BI0121813